BRILL

JOURNAL OF AFRICAN ARCHAEOLOGY 18 (2020) 209-228

brill.com/jaa

Robberg Material Procurement and Transport in the Doring River Catchment: Evidence from the Open-Air Locality of Uitspankraal 9, Western Cape, South Africa

Sara Watson
Department of Anthropology, University of California, 1 Shields Avenue, Davis, CA 95616, USA
sewatson@ucdavis.edu

Marika Low
Centre for Archaeological Science, School of Earth, Atmospheric, and Life Sciences, University of Wollongong, Northfields Ave Wollongong, NSW 2522, Australia

Natasha Phillips
Centre for Archaeological Science, School of Earth, Atmospheric, and Life Sciences, University of Wollongong, Northfields Ave Wollongong, NSW 2522, Australia

Corey O'Driscoll
Centre for Archaeological Science, School of Earth, Atmospheric, and Life Sciences, University of Wollongong, Northfields Ave Wollongong, NSW 2522, Australia

Matthew Shaw
Centre for Archaeological Science, School of Earth, Atmospheric, and Life Sciences, University of Wollongong, Northfields Ave Wollongong, NSW 2522, Australia

Chris Ames
Centre for Archaeological Science, School of Earth, Atmospheric, and Life Sciences, University of Wollongong, Northfields Ave Wollongong, NSW 2522, Australia
Department of Anthropology, University of Victoria, Cornett Building, B228, Victoria, BC, Canada

Zenobia Jacobs
Centre for Archaeological Science, School of Earth, Atmospheric, and Life Sciences, University of Wollongong, Northfields Ave Wollongong, NSW 2522, Australia
Australian Research Council Centre of Excellence for Australian Biodiversity and Heritage, School of Earth, Atmospheric, and Life Sciences, University of Wollongong, Northfields Ave Wollongong, NSW 2522, Australia

Alex Mackay
Centre for Archaeological Science, School of Earth, Atmospheric, and Life Sciences, University of Wollongong, Northfields Ave Wollongong, NSW 2522, Australia
Department of Archaeology, University of Cape Town, Beattie Building, Private Bag X3, Rondebosch 7701, South Africa

Abstract

Decisions related to the production of lithic technology involve landscape-scale patterns of resource acquisition and transport that are not observable in assemblages from any one single site. In this study, we describe the stone artifacts from a discrete cluster of stone artifacts assigned to the Robberg technocomplex (22-16 ka) at the open-air locality of Uitspankraal 9 (UPK9), which is located near two major sources of toolstone in the Doring River catchment of Western Cape, South Africa. OSL dating of the underlying sediment unit provides a *terminus post quem* age of 27.5 ± 2.1 ka for the assemblage. Comparison of near-source artifact reduction at UPK9 with data from three rock shelter assemblages within the Doring watershed – Putslaagte 8

 | DOI:10.1163/21915784-20200013

(PL8), Klipfonteinrand Rock Shelter (KFR), and Mertenhof Rock Shelter (MRS) – suggests that "gearing-up" with cores and blanks occurred along the river in anticipation of transport into the wider catchment area. The results reveal an integrated system of technological supply in which raw materials from different sources were acquired, reduced, and transported in different ways throughout the Doring River region.

Keywords

Robberg – Later Stone Age – open-air archaeology – lithic analysis – OSL dating – South Africa – Doring River Archaeology Project – Uitspankraal 9

Introduction

Archaeologists use the material culture record to understand how social and ecological factors influenced decisions of mobility and land use strategies and how those strategies changed over time. Cave and rock shelter sites often preserve stratified deposits which are used to construct culture history sequences and build hypotheses regarding past behaviors. However, individual sites capture snapshots of prehistoric technological organization within a larger system of material acquisition, production, transport, and discard. Because these sites are points within a system, no single site is able to provide data that encapsulates the system in its entirety. The importance of these sites within larger regional systems becomes more explicit when they are analyzed in combination with one another. Yet in southern Africa, and despite some important exceptions (Wilkins et al. 2017), single site descriptions continue to be used to model landscape-scale processes of lithic production and transport. This has led to a focus on discussions of local or non-local materials within an assemblage, with limited data on underlying systems of raw material extraction and transport. Lithic technology is an enduring record of human behavior that can survive depositional conditions in which organic materials will not, and in many instances it is the only remaining record of prehistoric lifeways. Lithic technological organization is based on the landscape-scale distribution and availability of resources, and the mobility systems used by past people are influenced by decisions of raw material acquisition and transport (Bamforth 1991; Nelson 1991; Kuhn 1992, 1995; Andrefsky 1994), making lithic technology a useful tool in understanding human landscape use and decision making.

The Doring River catchment in South Africa provides an opportunity to discuss technological organization within a regional system of landscape use. The region contains a rich late Pleistocene record of open-air and dated rock shelter assemblages with Middle and Later Stone Age (MSA and LSA) deposits. Researchers have used these assemblages to reconstruct landscape-scale patterns of tool production and transport in the late MSA (Will et al. 2015) and Early Later Stone Age (ELSA) (Low et al. 2017). In past studies of Robberg technology in the Doring River catchment, Low & Mackay (2018) suggested specific patterns of raw material acquisition, transport, and discard organized around the Doring River. However, the requisite data from near-source assemblages was not available at that stage to test resulting hypotheses. Here we describe the results of the analysis of a Robberg cluster at the open-air locality Uitspankraal 9 (UPK9) located on the Doring River and proximate to major toolstone sources. These new data builds on previous research and allows us to test and refine our previous model, adding important detail to our understanding of Robberg technological organization in the region.

Background

Southern African Later Stone Age

Technological systems associated with the LSA date back to >40 ka in southern Africa (Wadley 1993; Lombard et al. 2012; Villa et al. 2012; Bousman & Brink 2018). LSA assemblages are characterized by a lack of core technologies and tool types associated with the MSA, and a general – though not exclusive – focus on the production of small tools such as bladelets and scrapers from small cores (Deacon 1984; Wadley 1993; Lombard et al. 2012; Pargeter 2016). The LSA is subdivided into several distinct technocomplexes: the ELSA, Robberg, Oakhurst, Wilton, final LSA, and ceramic final LSA (Lombard et al. 2012). The ELSA and Robberg technocomplexes are often referred to as the "late Pleistocene microlithic" because of the systematic production of small tools from small cores, though they feature very different reduction systems (Deacon 1984; Wadley 1993; Lombard et al. 2012).

The ELSA is generally described as "highly variable" due to its diversity of features, though an emphasis on bipolar reduction is common (Mitchell 1988; Wadley 1993). Within the Doring River catchment, a regional variant focused on hornfels blade production was identified (Low et al. 2017). In contrast, Robberg technology is characterized by the production of bladelets from distinctive single platform cores, and a general lack of retouched implements

(Deacon 1984). Small lithics are replaced by large side-struck flakes in the subsequent Oakhurst technocomplex and do not reappear until the Wilton. Both the Oakhurst and Wilton, however, feature the regular production of scrapers, which are rare in preceding phases. Wilton assemblages also typically feature small backed pieces and geometrics (Deacon 1982, 1984). Final LSA assemblages are also described as highly variable with frequent occurrences of large unretouched flakes, backed artifacts, and adzes. Backed artifacts are still present in the ceramic final LSA, though in lower frequencies, along with low frequencies of retouched tools associated with pottery (Deacon 1984).

The Robberg Technocomplex

The Robberg technocomplex is known from cave and rock shelter assemblages across southern Africa. Robberg assemblages date to late Marine Isotope Stage (MIS) 2 (Deacon 1984; Mitchell 1988, 1995; Loftus et al. 2016; Pargeter et al. 2017, 2018). The earliest dated Robberg assemblages are found at the sites of Sehonghong (25.7-24.4 ka) and Heuningneskrans (25.4-23.9 ka), suggesting a possible origin of the technocomplex in the eastern interior of southern Africa (Vogel et al. 1986; Mitchell 1996; Bousman & Brink 2018). Recent redating of Robberg layers from Nelson Bay Cave on the south coast to ~23.4-22.6 ka suggests that the spread of this technology must have been relatively rapid (Loftus et al. 2016).

Robberg technology is characterized by the production of bladelets from volumetric single platform cores. Bladelets are defined by Deacon (1984) as flakes with parallel sides, a length greater than twice the width, and a maximum width of 12 mm. Raw material preferences for the production of Robberg technology often favor fine-grained and crystalline materials such as quartz, chert, and silcrete (Deacon 1978, 1984; Mitchell 1988, 1995; Wadley 1993). Many assemblages also have a notable occurrence of bipolar technology in addition to volumetric bladelet production in the form of bipolar cores, flakes, and *pièces esquillées*. Bipolar reduction was used most often with quartz or chert (Deacon 1982; Pargeter 2017). Bladelets are generally unretouched, while retouched tools are relatively rare and typically comprise <1% of the total assemblage when all materials are considered regardless of size (Deacon 1978, 1984; Mitchell 1988, 1995; Wadley 1993).

The role of lithic provisioning strategies within the Robberg has been considered in a number of studies over the last few decades. Bladelet cores are more common than bladelets in assemblages from some sites, potentially indicating the independent transport of different elements within the toolkit (Deacon 1984; Mitchell 1988; Barham 1989; Wadley 1993; Low & Mackay 2018). Sehonghong in the Lesotho highlands and Boomplaas in the Cango Valley both preserve evidence for the transport of unworked lithic raw materials and small, lightweight "working cores" (Pargeter 2017; Chase et al. 2018). Similar evidence for the transport of lightweight cores was documented in the Caledon Valley as well (Mitchell 2000), suggesting that transport of lithic manufacturing potential – or place provisioning (Kuhn 1995) – might have been a widespread feature of Robberg technological systems.

The Doring River Catchment

The Doring River catchment east of the Cederberg Mountains in South Africa provides an opportunity to explore these ideas further, but more importantly to understand how spatially separated artifact accumulations fit into larger systems of lithic technological organization. The catchment contains numerous rock shelter sites and open-air lithic concentrations, coupled with distinct patterns of raw material availability, providing the data needed to examine factors influencing technological organization and decision-making (Shaw et al. 2019) (Fig. 1). Robberg assemblages have been documented at several rock shelters (Low & Mackay 2016, 2018; Low 2019), with ages between 22.3 ka and 16.3 ka (Mackay et al. 2020). These assemblages are characterized by elevated proportions of silcrete relative to all other LSA technocomplexes, frequent single platform cores <20 g, common blades and bladelets, and a persistent bipolar component dominated by quartz. Most of the laminar pieces in these assemblages could be classed as bladelets (Low 2019), however, the continuous nature of the metric data of these pieces rendered any distinction between blades and bladelets arbitrary and thus not technologically meaningful (Low & Mackay 2018).

Skirting this distinction, Low & Mackay (2018) undertook an analysis of blades and blade cores from Robberg levels at three rock shelter sites – Putslaagte 8 (PL8), Klipfonteinrand (KFR) and Mertenhof (MRS) – located at increasing distances from the Doring River. They found that the abundance of hornfels and silcrete blades decayed with distance from the Doring River channel, with an increasing use of locally available quartz. Increasing blade to blade core ratios also suggested that blades were more commonly transported than the cores used to produce them. Low & Mackay (2018) also found that while silcrete and hornfels blade cores became smaller with distance from the river, silcrete cores occurred in consistent frequencies at all distances, suggesting their transport

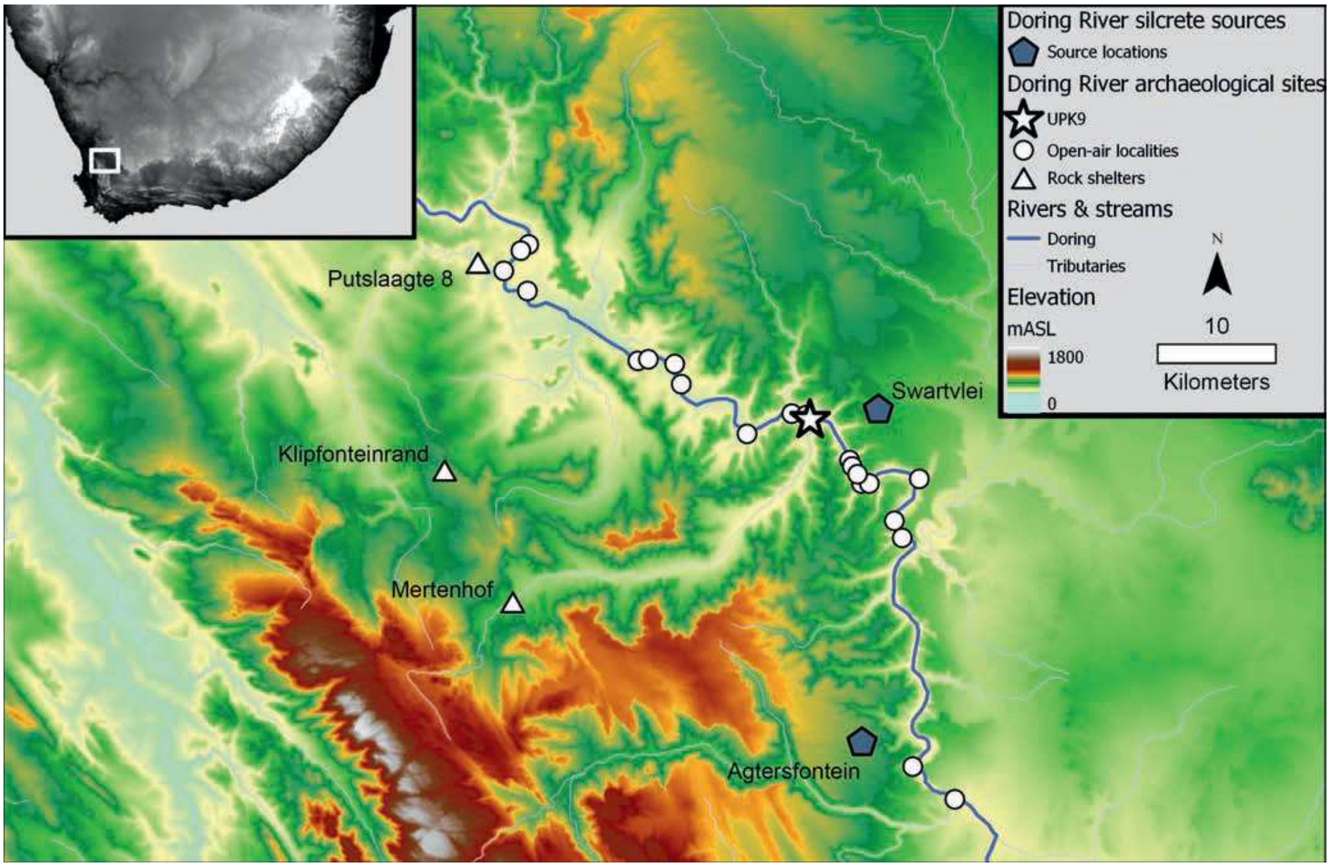

FIGURE 1 Study area showing open-air and rock shelter localities in addition to known silcrete sources

throughout the catchment as working cores, in line with findings from Sehonghong and Boomplaas (Pargeter 2017). Hornfels blade cores, on the other hand, were never frequently transported to the sites analyzed. The results led Low & Mackay (2018) to posit an organizational system involving the production of silcrete and hornfels blades at locations on the Doring River, and the subsequent transport of those blades and silcrete working cores into other parts of the catchment area.

Weakening this hypothesis was the absence of data from Robberg assemblages located on the Doring River itself, inferred to be a key point in the system. The hypothesis does, however, present clear test conditions for the expected composition of such an assemblage near the river. Specifically, the assemblage should retain an abundance of silcrete and hornfels blades and blade cores with relatively low proportions of quartz. Signs of early stage reduction, including primary or near-primary flakes and blades, are expected, and silcrete and hornfels blade cores should be larger than comparable artifacts from the rock shelter assemblages analyzed by Low & Mackay (2018). The open-air locality UPK9 provides an opportunity to test these propositions. Mapped and analyzed as part of the on-going Doring River Archaeology Project (DRAP) (Shaw et al. 2019), UPK9 contains a wealth of Robberg artifacts in three clusters spread across an extensive area of the locality. Here we focus on artifacts from one cluster eroding out from above an indurated sediment unit for which we have one optically-stimulated luminescence (OSL) age. We first describe the locality, its geological and geomorphic contexts, and our analytic methods.

Uitspankraal 9 (UPK9)

UPK9 is an open-air archaeological locality situated near the confluence of the Biedouw and Doring Rivers. The locality is an eroding aeolian sediment stack positioned on a gentle slope approximately 15-30 m in elevation above the Doring River, and 160 m north of the active river channel. The Doring River is the major source of hornfels in the study area, with artifacts typically manufactured on cobbles extracted from the bedload of the river (Low & Mackay 2018). Cobbles of the pedogenic rock silcrete are also present in the Doring River cobble beds, though these were exploited comparatively rarely. The nearest primary source of silcrete is at Swartvlei, located on an elevated plateau 4.5 km east and 220 m above UPK9 (Fig. 1). UPK9

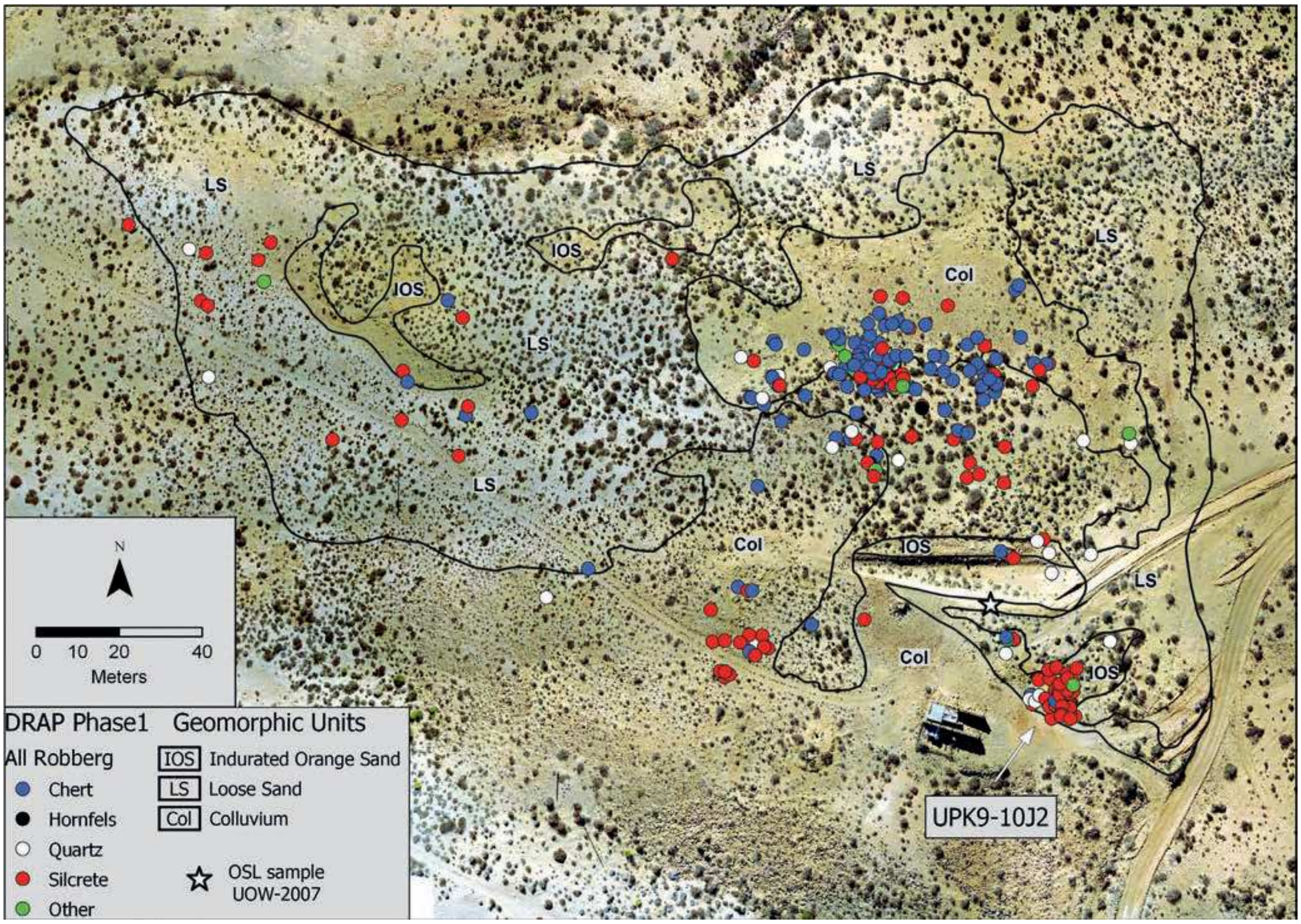

FIGURE 2 Robberg artifacts at UPK9 by raw materials in relation to major geomorphic units

is thus located significantly closer to the sources of these two major raw materials compared to the assemblages from the three sites analyzed by Low & Mackay (2018).

Initial geomorphic and archaeological mapping of UPK9 was undertaken between 2018 and 2019, as part of the DRAP, a three-phase project focused on the open-air archaeology of the Doring River catchment. Geomorphically, UPK9 comprises four broadly defined sediment units, three of which are exposed in a cutting in the south-eastern corner of the locality (Figs. 2 and 3). The oldest unit is a basal calcrete restricted to the south-eastern corner and dating to approximately 220 ka (Shaw et al. 2019). Overlying this is an indurated orange sand which is again prevalent in the south-eastern corner though appears to extend further to the north and across much of the site including the western half. A well-defined coarse colluvium separates the basal calcrete and the indurated orange sand, suggesting a significant amount of time elapsed between the overlying and underlying units (Fig. 3). The youngest unit is a modern aeolian sand preserved only in vegetated areas; as with all other mapped sediment stack localities on the Doring River, sediment preservation is contingent on remnant vegetation, with erosion aggressively transforming them under modern climatic and land-use conditions (Ames et al. 2020a).

Phase 1, which involved mapping and limited in-field analysis of cores and implements (with no size cut-off) on a mobile GIS platform (Ames et al. 2020b), resulted in the identification of 9486 artifacts at UPK9 (Shaw et al. 2019). While artifacts from the Earlier Stone Age (ESA), Middle Stone Age (MSA), Later Stone Age (LSA) and Iron Age periods were all present, LSA artifacts dominated the locality, with clusters of artifacts relating to the Wilton, Oakhurst, and Robberg all identified. Assignment to these technocomplexes was based on their key identifying characteristics as summarized in the brief review above, and by comparison to a regional reference collection developed from the excavated and dated Doring River rock shelter assemblages as discussed in Shaw et al. (2019). With respect to the Robberg, identifying features were the elevated proportion of silcrete, common single platform volumetric cores, frequent laminar products (bladelets grading into blades), infrequent retouched pieces, and a persistence of quartz bipolar cores. By comparison,

FIGURE 3
Location of OSL sampling and sedimentary units. (A) Context of OSL sample relative to the cluster at UPK9-10J2. Note that the structure visible in the center of the image is the same as that shown in the bottom right of Figure 2. (B) Placement of sample relative to indurated orange sand, colluvium and calcrete-rich sediment. (C) Sampling location showing depth below current surface. (D) Close-up image of sampling location noting presence of bioturbation (termite activity)

Wilton assemblages at UPK9 were distinguished by the frequency of small scrapers and backed pieces that were absent from the Robberg clusters. Other than a few isolated artifacts scattered on the western half of the locality, most Robberg artifacts occur in three clusters on the eastern half: two composed mostly of silcrete and one with high proportions of chert (Fig. 2).

In 2018, the DRAP undertook a Phase 2 analysis of artifacts from the southernmost Robberg cluster (Fig. 4), denoted UPK9-10J2. This cluster was selected because it is spatially coherent and has limited evidence for incorporation of older or younger components, and because it is underlain by a datable sediment unit – the indurated orange sand – from which a single OSL sample (FieldID 91082; LabID UoW-2007) was extracted from the cutting. In contrast, the other two Robberg clusters were disaggregated by erosion (second silcrete cluster) or deflated onto the underlying colluvium (chert cluster).

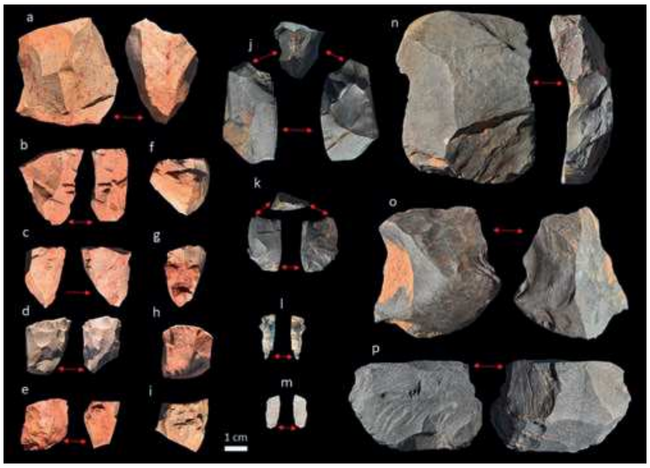

FIGURE 4 Selection of Robberg artifacts from UPK9-10J2. (a-i) freehand silcrete cores, (j, k) bipolar hornfels cores, (l, m) bipolar quartz cores, and (n-p) freehand hornfels cores

Methods

Phase 2 of the DRAP involved analysis of all artifacts within an identified cluster, with a size cut-off of >20 mm maximum dimension applied to all pieces other than retouched flakes and cores (Low et al. 2017; Shaw et al. 2019). This cut-off is used for several reasons. Foremost, all artifacts are field-analyzed and replaced in-situ to minimize impact on the archaeological resource. In the absence of excavation and screening, however, the artifact recovery rate below 20 mm is assumed to be highly variable within and between analysts. Secondary concerns are pragmatic: due to the abundance of material at the Doring River localities, the high search time for very small artifacts, and the fact that mapping, analysis and post-analysis replacement of artifacts takes place on site, the time costs associated with analyzing fragments of all sizes is simply too high to be viable. These points made, the use of arbitrary size cut-offs unquestionably creates complications when comparing to excavated assemblages that we discuss later.

At UPK9-10J2 each artifact was flagged and given a unique identifier, mapped with a Trimble RTK GNSS system, analyzed and then replaced. Artifact class, lithic raw material, cortex type, cortical coverage, mass, and maximum metric dimensions (length, width, and thickness) were recorded for all artifacts, regardless of completeness. Mass was recorded to the nearest tenth of a gram (g), and metric data was recorded to the nearest hundredth millimeter (mm) using standard digital calipers with a USB connection. Additional attributes were recorded to characterize variability within the assemblage. These attributes were used to examine the intensity of reduction that occurred and the phases of the reduction sequence that are present in the assemblage, and to understand the reduction methods and techniques that were used during production. For the flake assemblage, these attributes include flake scar counts, flake scar patterns, cortical coverage, and artifact size data. Attributes recorded for the core assemblage include the number of striking platforms utilized during reduction, the primary flaking product (flakes or blades), the number of previous removals preserved, and the patterning of previous removals.

Following Low & Mackay (2018), whose hypothesis we are testing, no *a priori* distinctions were made between blades and bladelets (*sensu* Pargeter & Redondo 2016). Blades are defined as flakes with parallel sides and maximum axial length at least twice as long as they are wide. Blade cores are defined as cores which preserve evidence of at least one blade removal at the time of discard. Cortex coverage was used to assess the degree of reduction, the presence or absence of different parts of the reduction sequence, and whether cores were reduced on site or finished products were transported into the locality. Flake scar counts were used as a proxy for the intensity of reduction and scar patterns provide information on the direction of removals and the number of potential core rotations. Metric data was also used as a proxy of reduction intensity. Flakes produced during the initial stages of core reduction will generally be larger than those produced closer to exhaustion or discard of a core. Comparisons of metric data can also be used to infer patterns of transport or raw material-specific differences in reduction intensity.

Models of reduction strategies were created using principles for the reconstructions of *chaîne opératoires*, which describe the series of transformations, from material selection and procurement to discard, of culturally modified materials such as lithics (Leroi-Gourhan 1964, 1965; Tixier 1980; Boëda et al. 1990). The reconstruction of reduction sequences combines quantitative data with qualitative observations to create models that provide understanding of the processes at work during lithic reduction. This approach can provide insight into any differences in the treatment of raw materials and how much of the production sequence occurred on site. It can also facilitate comparisons between assemblages to understand the degree of variation present within Robberg technology across southern Africa and how this relates to other aspects that may influence technological decision making, such as site setting and resource distribution. Given the limitations of the sample, a full *chaîne operatoire* was not reconstructed.

As noted, a 20 mm size cut-off was applied to all artifacts except cores and retouched flakes. Low et al. (2017) assessed the potential of the 20 mm cut-off to introduce bias in a study of ELSA artifacts from the nearby locality Uitspankraal (UPK7), which is separated from UPK9 by a drainage channel, but found no significant difference in assemblage composition between samples analyzed with and without size cut-offs. To some extent this probably reflects the recent exposure of artifacts in the ELSA cluster at UPK7; within decadal intervals of exposure we expect the loss of the finer artifact fraction based on our experimental studies (Phillips et al., 2019). Duration of exposure of UPK9-10J2 is unknown but given its coherence we expect it to have been exposed fairly recently. In spite of these caveats, the arbitrary size cut-off complicates comparison of our results with those of Low & Mackay (2018), particularly with respect to the blade component of the UPK9 assemblage. A large majority (76%) of the blades recorded in their analysis were <20 mm, meaning that the two populations cannot be directly compared in these terms. For that reason, our treatment of the blade and flake data from UPK9 will be relatively descriptive, and our focus will largely be on the results of the core analysis. A detailed description of the UPK9 assemblage is presented before comparing trends in technological organization with Robberg assemblages from the sites previously recorded by Low & Mackay (2018).

As a result of small sample size and exposure to the elements, the potential for mixing at UPK9-10J2 is a matter of concern. There is limited evidence for older or younger material at UPK9-10J2 and assemblages assigned to other LSA technologies, such as Oakhurst and Wilton, have not been identified in the vicinity of this cluster. The potential for within technocomplex mixing is more difficult to reconcile. Components of the UPK9-10J2 assemblage may not have formed contemporaneously, a matter we address further later in the paper. Therefore, we focus on the identification of larger behavioral patterns and systems of artifact production and transport, which may be more easily identified in time-averaged aggregates (Barton & Riel-Salvatore 2014).

Results

Sedimentology and OSL Dating

A single sample for OSL dating (UoW-2007) was collected from an indurated orange sand unit, approximately 14 m north of the UPK9-10J2 cluster (Fig. 3A-D). This unit overlies a horizon of artifact-rich colluvium and a basal deposit of calcrete-rich sediment (Fig. 3B-D). Based on macro-scale observation, the indurated orange sand unit shows the absence of depositional structure and the presence of fine roots and small vesicles, suggesting possible bioturbation of this unit. This is further suggested by the presence of termite activity below the sampled sediment, indicated in Figure 3D. The sediment is a sandy loam (69% sand, 26% silt, 5% clay (<4 μm)) and dominated by quartz (83%) and some feldspars (12%). Detrital clay minerals (~5%) are a possible indication of minor secondary weathering of very fine grains (e.g. feldspar and dolerite). The mineral and particle composition of the sediment is consistent with aeolian deposits from the adjacent UPK7 locality. The sediment was sampled using a stainless-steel tube (Fig. 3C) and the 180-212 μm-diameter quartz grains were extracted and prepared following standard laboratory procedure (Wintle, 1997) under dim red-light in the University of Wollongong Optical Dating Laboratory.

Standard measurement equipment was used for estimation of the sample's equivalent dose. Using a Risø DA-20 TL/OSL reader, 1000 individual quartz grains were measured using the single aliquot regenerative-dose (SAR) procedure (Murray & Wintle 2000) to estimate the equivalent dose (D_e). PH_1 and PH_2 temperatures of 240°C for 10 s and 160°C for 5 s were used prior to measurement of all regenerative and test dose measurements, respectively. Aberrant grains were rejected using quality-assurance criteria, resulting in 43 accepted grains for which individual D_e values could be calculated. Most grains (n = 890) had no inherent signal or signals, and were thus too dim to be detected. Figures 5A-C show decay curves for 10 accepted grains following measurement of the largest regenerative dose and an example dose response curve for one representative grain.

The distribution of all D_e values (n = 43) are presented in a radial plot in Figure 6 (Galbraith et al. 1999). The single-grain D_e distribution is over-dispersed (OD) by 44 ± 2%. Two outliers (shown as open triangles) were identified using the normalized median absolute deviation (nMAD) (Rousseeuw et al. 2006; Wood et al. 2016). After their exclusion, the OD reduced to 33.9 ± 5.2%. We used the Central Age Model of Galbraith et al. (1999) to calculate a single weighted mean D_e of 50.6 ± 3.4 Gy for age calculation.

We estimated the beta dose rate of 0.97 ± 0.04 Gy/ka directly by low-level beta counting following the procedures described in Jacobs & Roberts (2017), making allowance for attenuation due to grain size (Mejdahl 1979; Brennan 2003). The gamma dose rate of 0.63 ± 0.04 Gy/ka was derived from U (2.08 ± 0.08 ppm), Th (3.93 ± 0.64 ppm) and K (0.98 ± 0.05%) concentrations obtained using a combination of thick source alpha counting and beta counting.

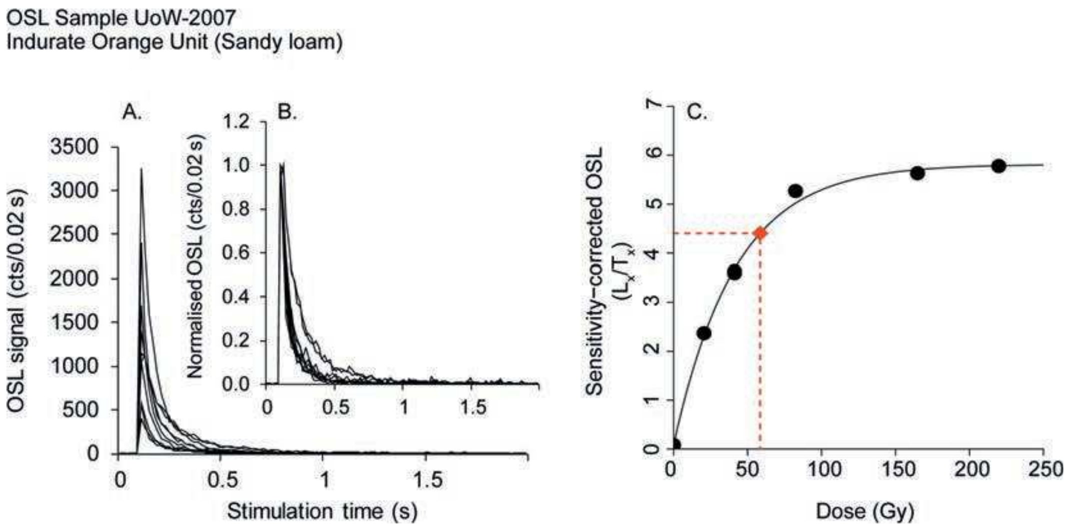

FIGURE 5 Single-grain OSL decay (A and B) and a dose response (C) curve(s) for UoW-2007. (A) depicts a representative sample of OSL decay curves showing a range of luminescence sensitivities for 10 grains. The normalized signals for the same grains are shown in (B). (C) shows a typical dose response curve for one of these grains.

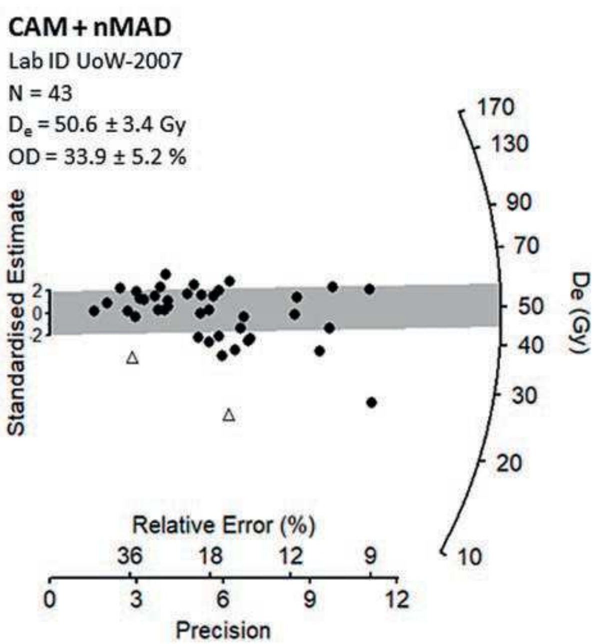

FIGURE 6 Radial plot of D_e distribution for accepted quartz grains for OSL sample UoW-2007. The grey band is centered on the weighted mean determined using the Central Age Model (CAM) after identification and rejection of two outliers (open triangles) using nMAD.

An allowance for attenuation of the beta and gamma dose rates due to moisture (Aitken 1985) in the sample was also made, assuming a long-term water content of 5.0 ± 1.3%. The cosmic-rays contribution was determined from the sample's altitude (209 m asl), geomagnetic latitude (−30.9), sediment density (1.8 g/cm^3) and depth below deposit surface (0.65 m, accounting for historic erosion) (Prescott & Hutton 1994). An internal alpha dose rate of 0.03 ± 0.01 Gy/ka was assumed. The uncertainty on the total dose rate was calculated by summing all systematic and random errors in quadrature, resulting in a total dose rate of 1.83 ± 0.06 Gy/ka.

The OSL age was calculated by dividing the D_e (50.6 ± 3.4 Gy) by the total dose rate (1.83 ± 0.06 Gy/ka) to provide a depositional age estimate of 27.5 ± 2.1 ka for the indurated orange sand. This is a maximum age for the overlying Robberg archaeology of UPK9-10J2.

UPK9-10J2 General Assemblage Composition

We analyzed 675 artifacts from UPK9-10J2. Flakes (53%) comprise the majority of the assemblage (Table 1), with cores well represented (14%). Retouched flakes (3%) are more common than is typical of Robberg technology (Deacon 1978; Mitchell 1988; Wadley 1993), though still within the range of published variation (Porraz et al. 2016; Bader et al. 2020). The relatively high frequency of retouched tools as well as cores in our assemblage likely results from the exclusion of unretouched flaked products <2 cm (Bader et al. 2020). Nonflaked lithic artifacts occur in low frequencies, comprising hammerstones (0.7%), unmodified river cobbles (0.4%), and unmodified ochre nodules (0.3%). The rest of the assemblage is comprised of flaked pieces and heat shatter, the latter exclusively on silcrete. There is some evidence for recent taphonomic processes, as 7% of artifacts have fresh edge damage.

UPK9-10J2 Raw Material and Cortex

Hornfels is the dominant material within the UPK9-10J2 assemblage (53%), followed by silcrete (20%) (Table 1). Quartzite, quartz, and 'other' materials are present in low

TABLE 1 Summary of assemblage composition by raw material and artifact class, including completeness

	Hornfels	Quartz	Quartzite	Silcrete	Other	Total
Core						
Complete	30	13	7	33	6	89
Broken	5	1	0	0	0	6
Flake						
Complete	108	5	24	52	11	200
Broken	77	10	33	33	7	160
Retouched flake						
Complete	7	2	0	0	2	11
Broken	8	0	1	3	0	12
Flaked piece						
Complete	104	20	22	8	12	166
Broken	14	0	0	2	0	16
Nonflaked lithic	2	1	3	0	4	10
Heat shatter	0	0	0	5	0	5
Total	355	52	90	136	42	675

frequencies, with quartz accounting for only 8% of the assemblage total.

The assemblage is characterized by a high degree of cortex. Over half of all hornfels (52%), silcrete (52%), and quartz (55%) artifacts have some cortex. Cores with >50% cortex can be found of hornfels (7%), quartzite (4%), and silcrete (1%). Early stage flakes with >75% cortex are present across all materials, but are most frequent in hornfels (6%) and silcrete (3%).

Consistent with prior observations and local availability of cobbles, 92% of the cortex on hornfels artifacts is of fluvial origin, with a further 6% of uncertain origin; only 2% of hornfels pieces had cortex suggestive of procurement from a primary source. Conversely, but again consistent with prior observations on other assemblages in the catchment, most of the cortex on silcrete artifacts reflects acquisition from primary sources (76%). Yet 22% of silcrete artifacts have fluvial cortex, suggesting considerable use of local, river-sourced cobbles as well. Among the other major raw materials, quartzite artifacts were mainly derived from river cobbles (62%), while quartz artifacts were sub-equally derived from primary sources (crystal surfaces on 50%), or as pebbles obtained from the river or conglomerate sources in the Table Mountain Sandstones (44%).

UPK9-10J2 Flaking Pattern – Complete Flakes

Flaking patterns and platform morphology for complete flakes and retouched flakes are summarized in Table 2. Flakes from all stages of production are present across raw material types, as shown through cortex coverage. Most of the flakes have plain platforms, between 1-3 dorsal scars from previous removals, feather terminations, and unidirectional flake scars. This is consistent with published descriptions of Robberg technology, which is focused on volumetric bladelet production from unprepared single platform cores (Deacon 1978; Wadley 1993; Mitchell 1995). Bidirectional removals are slightly more frequent in silcrete artifacts than other materials, as are overshot removals. Silcrete flakes more frequently preserve higher dorsal scar counts than other raw materials, with 33% of flakes retaining 4-6 dorsal scars. Maintenance products such as crested blades and core tablets are absent from the sample.

UPK9-10J2 Flaking Pattern – Complete Cores

Attribute data for complete cores are summarized in Table 3. Cores of all stages of reduction are present in the assemblage, though early stage cores (>50% cortex) occur at low frequencies in most raw materials. Most cores retain some cortex, have one or two striking platforms, single platform or minimal removal patterns, and a focus on flake production. Equal proportions of cores (33%) have between 1-3 flake scars and between 4-6 flake scars. There is variation in the treatment of different materials, most notably in silcrete. Silcrete cores were used to produce blades, while most of the assemblage is driven by flake production. Silcrete cores are more intensively reduced, with 46% of silcrete cores preserving 7 or more flake scars.

TABLE 2 Attributes of complete flakes and retouched flakes by raw material

Attribute	Hornfels	Quartz	Quartzite	Silcrete	Other	Total
Cortex						
0%	41	3	5	27	5	81
1-50%	51	3	12	17	6	89
50-100%	23	1	7	8	2	41
Scar count						
0	11	0	2	4	1	18
1-3	62	6	18	28	9	123
4-6	38	1	3	17	3	62
7+	4	0	1	3	0	8
Scar pattern						
Unidirectional	61	4	14	32	7	118
Bidirectional	31	2	4	16	4	57
Centripedal	2	0	0	2	0	4
Polydirectional	6	0	0	1	1	8
Indeterminate	15	1	6	1	1	24
Platform type						
Cortical	3	0	0	0	0	3
Plain	67	1	21	41	5	135
Dihedral	5	1	0	3	1	10
Facetted	5	0	1	1	1	8
Linear	6	0	0	1	1	8
Punctiform	3	1	0	2	0	6
Crushed	7	3	0	0	0	10
Other	19	1	2	4	5	31
Termination type						
Feather	60	3	17	36	9	125
Hinge	32	0	3	0	1	36
Step	3	0	0	1	0	4
Overshot	13	1	4	14	1	33
Bipolar	6	2	0	0	0	8
Indeterminate	1	1	0	1	2	5

UPK9-10J2 Artifact Size

Table 4 summarizes the metric measurements for all complete flakes and blades, then for complete blades only and cores. When considering the means, hornfels and quartzite flakes (in the broad sense, comprising all flakes, blades and bladelets) show similar tendencies. Hornfels flakes are the longest, widest, and thickest while quartzite flakes are the heaviest. Silcrete and quartz flakes are also very similar to one another, with quartz flakes being the lightest, narrowest, and thinnest. Silcrete flakes are typically the shortest of the assemblage.

When restricted to blades, we see the same general pattern – hornfels and quartzite blades are larger than silcrete and quartz blades – however these metrics reveal two additional pertinent points. First, the mean width of silcrete blades is ~13.6 mm, at the approximate boundary between blades and bladelets as conventionally defined. That is, roughly half of the silcrete blades in the sample could be classed as bladelets, but as with previous work in the region (Low 2019), the conventional distinction here is essentially meaningless. If it has any utility it would be in suggesting that hornfels and quartzite blades less often conformed to bladelet dimensions, but that observation is evident from the metrics alone without recourse to arbitrary distinctions. Furthermore, given that the mean length for silcrete blades is extremely close to the 20 mm cut-off, it is likely that many of the artifacts that would conventionally be classed as bladelets are missing from

TABLE 3 Attributes of complete cores by raw material

Attribute	Hornfels	Quartz	Quartzite	Silcrete	Other	Total
Cortex						
0%	6	7	0	9	2	24
1-50%	19	6	3	23	4	55
51-100%	5	0	4	1	0	10
Number of platforms						
1	11	4	4	17	4	40
2	15	8	3	13	2	41
3	4	1	0	2	0	7
4+	0	0	0	1	0	1
Flake scars						
1-3	13	5	3	6	2	29
4-6	11	7	2	11	2	33
7-9	4	1	0	13	2	20
10+	2	0	2	3	0	7
Primary product						
Flakes	30	8	7	2	3	50
Blades	0	5	0	30	3	38
Removal pattern						
Single platform	3	2	3	22	2	32
Prepared core	4	1	0	2	1	8
Minimal	12	2	3	1	2	20
Other	9	4	0	4	0	17
Indeterminate	2	4	1	4	1	12

TABLE 4 Metric measurements for all complete flakes, complete blades, and complete cores by raw material

			Mass			Length			Width			Thickness		
Class	**Material**	**N**	**Mean**	**SD**	**Median**	**Mean**	**SD**	**Median**	**Mean**	**SD**	**Median**	**Mean**	**SD**	**Median**
All complete flakes & blades	**Hornfels**	115	12.42	13.96	6.9	39.76	13.19	37.48	26.35	10.12	25.51	9.23	5.38	8.16
	Quartz	7	2.17	1.38	1.4	26.63	4.94	24.27⍰	12.17	3.61	9.41	5.53	1.89	5.61
	Quartzite	24	14.06	18.31	6.15	38.91	14.97	37.11	24.8	12.01	18.99	9.95	4.93	8.91
	Silcrete	52	2.86	3.66	2.1	25.02	5.97	23.3	16.42	5.97	15.37	6.18	2.59	6.07
	Other	13	11.52	16.83	5.4	34.49	15.75	30.56	22.4	11.63	18.73	9	5.05	7.34
Blades only	**Hornfels**	33	13.25	16.15	5.4	39.34	15.38	34.15	24.91⍰	11.22	25.25	9.57	4.86	8.09
	Quartz	5	2.14	1.3	1.4	25.41	3.57	27.89	11.76	3.12	10.76	5.84	1.51	5.53
	Quartzite	11	10.1	12.7	5.9	37.56	12.58	37.69	22.88	9.69	18.56	8.86	5.06	7.08
	Silcrete	28	1.86	1.18	1.5	23.69	3.76	22.81	13.67	4.02	13.62	5.38	2.54	4.93
	Other	9	6.26	6.33	2.2	33.91	16.68	27.92	22.48	13.47	16.34	8.03	4.85	7.34
Complete cores	**Hornfels**	30	117.71	228.62	73.15	63.99	22.17	64.92	45.75	15.71	47.73	24.1	12.41	22.65
	Quartz	13	5.31	6.1	2	22.42	9.47	20.79	13.57	6.65	12.21	9.8	6.2	6.65
	Quartzite	7	510.5	264.5	478	108.04	30.85	108.43	75.86	21.06	75.18	49.07	12.95	52.38
	Silcrete	33	14.12	13.2	11.1	31.33	7.97	29.53	24.49⍰	7.54	22.51	16.76	5.11	15.1
	Other	6	35.83	52.2	5.3	42.11	22.47	28.36	29.42	16.69	21.57	11.2	7.34	8.98

TABLE 5 Comparison of blade and flake frequencies in flake and core assemblages by raw material, regardless of completeness

Class	Material	Total	Flakes	%	Blades	%
Flakes	Hornfels	200	104	52.00	96	48.00
	Quartz	17	3	17.65	14	82.35
	Quartzite	57	22	38.60	35	61.40
	Silcrete	88	33	37.50	55	62.50
	Other	20	8	40.00	12	60.00
	Total	382	170	44.50	212	55.50
Cores	Hornfels	35	35	100.00	0	0.00
	Quartz	14	9	64.29	5	35.71
	Quartzite	7	7	100.00	0	0.00
	Silcrete	33	3	9.09	30	90.91
	Other	6	3	50.00	3	50.00
	Total	95	57	60.00	38	40.00

the sample. This reinforces our analytic emphasis on the core rather than the flake fraction.

UPK9-10J2 Blade Technology

Blades comprise 56% of the flake assemblage at UPK9-10J2, regardless of completeness (Table 5). They are the most common product across raw materials except for hornfels, for which flakes are slightly more common. Silcrete blades are the lightest, thinnest, and shortest within the assemblage while hornfels blades are the heaviest and largest (Table 4). Blades from all stages of production are present for hornfels, quartzite, and silcrete, including completely cortical blades from the initial stages of core reduction. Early reduction stage blades, i.e. those which preserve >75% cortex, also occur on quartz.

Despite the prevalence of blades within the assemblage, most cores from UPK9-10J2 primarily have flake detachment scars (Table 5). Silcrete cores depart strikingly from this pattern, though, with over 90% discarded at a stage where blades were the primary product. Interestingly, no hornfels cores with blades as the primary product were recorded, despite the relative abundance of hornfels blades. Only one in seven hornfels cores has blade scars.

UPK9-10J2 Bipolar Technology

There is limited evidence for the use of bipolar technology in the UPK9-10J2 assemblage. Bipolar artifacts comprise only 7% of the entire assemblage. It is possible that the paucity of bipolar flakes is a result of the 20 mm size cut-off. No such size cut-off was used for cores; it is thus likely that the core sample reflects the frequency with which these appear at the locality. Evidence of bipolar reduction is limited to hornfels, quartz, and 'other' materials. Most bipolar flakes were made from hornfels (80%), but most bipolar cores were made from quartz (50%). Given that most quartz cores are close to 20 mm when discarded, it is likely that the proportion of quartz bipolar flakes is being underestimated due to our analytical cut-off.

UPK9 Reduction Systems

Reduction systems were reconstructed for hornfels and silcrete artifacts to assess the treatment of at-source (hornfels) and near-source (silcrete) materials, and to evaluate how the production systems present at UPK9-10J2 fit into the broader landscape-scale patterns already documented in the Doring River catchment.

Hornfels is the most common material in the assemblage. Hornfels flaked pieces and broken artifacts are relatively common within the assemblage. Completely decortified artifacts are present, but most preserve at least some cortex. Early stage flakes and cores indicate that the initial stages of lithic production occurred on site. Production seems to be informal with minimal investment. Hornfels cores are predominantly minimal cores (three or fewer removals) utilizing 1-2 platforms formed by natural convexities of the cobble. Evidence from the flake assemblage supports this pattern of low investment in hornfels reduction. Hornfels flake platforms are mostly unprepared, and the flakes have low dorsal scar counts with primarily unidirectional removal patterns. Most hornfels flakes at UPK9-10J2 have feather terminations, but hinge fractures and overshot removals are not uncommon. While the evidence for bipolar reduction is relatively rare, most bipolar flakes are hornfels. Blades, common in Robberg technology, comprise just under half of all hornfels flakes, but evidence for blade production on hornfels cores is largely incidental.

Silcrete is the next most common material in the UPK9-10J2 assemblage. The silcrete flake assemblage is about half as large as hornfels, but there are only two fewer silcrete cores than hornfels. There are some early stage silcrete flakes and cores, and this includes a reasonable proportion of the blades in the sample (15% of silcrete blades have >50% cortex), consistent with the establishment of blade cores on site. Reduction patterns on silcrete differ from those observed in hornfels and are more typical of Robberg technological strategies. Silcrete cores are primarily unidirectional single platform cores utilizing 1-2 platforms and are more heavily reduced than hornfels, with silcrete cores averaging 4-9 removal scars. These patterns are supported by the flake assemblage, with most platforms being unprepared and flakes preserving 1-6 scars from previous removals. These removals are most frequently unidirectional, but bidirectional removals are more common among silcrete than any other raw material. Feather terminations are the most common, but overshot removals are frequent, potentially reflecting the on-site establishment or management of axial core face convexities. There is no evidence for bipolar reduction on the silcrete flakes or cores. Blades comprise over 60% of the silcrete flake assemblage at UPK9-10J2, and nearly all silcrete cores (91%) are blade cores.

Landscape-Scale Patterns in Blade Cores

We compared blade cores from UPK9-10J2 with those from the local rock shelter sites of PL8, KFR, and MRS to understand how distance from raw material sources affects the treatment of the material during lithic production and transport. These sites are located at distances of 0.2 km (UPK9-10J2), 2 km (PL8), 13 km (KFR), and 19 km (MRS) from the Doring River. Cores are less likely to be affected by post-depositional transport than flakes (Phillips et al. 2019) and were not subject to size cut-off during analysis, so comparing core technology between assemblages is most likely to reflect landscape-scale patterns in technological organization. We examined evidence related to blade core size, production stages, and reduction intensity to understand the local landscape organization of Robberg blade technology. Note that following Low & Mackay (2018), we define ‘blade core’ here as any core that retains some evidence of having produced blades, whether they constituted a primary product of reduction or not.

The proportion of hornfels blade cores in the UPK9-10J2 assemblage is consistent with those at sites more distant

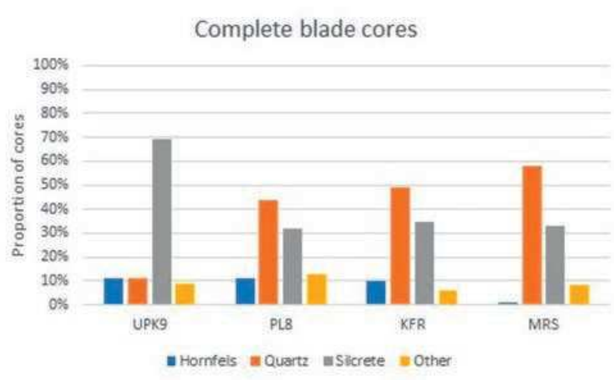

FIGURE 7 Proportion of complete blade cores for major raw materials at UPK9-10J2, PL8, KFR, and MRS

from the river, despite the local availability of hornfels cobbles for lithic production and the prevalence of hornfels artifacts at UPK9-10J2 (Fig. 7). Silcrete makes up over 68% of all blade cores at UPK9-10J2 – more than double its frequency in the rock shelter sites – while the proportion of quartz blade cores exhibits the opposite trend, being far less common at UPK9-10J2 than elsewhere. A chi-square test of association shows no statistically significant association between raw material and site for blades but does show association between raw material and site when considering blade cores (chi-square = 36.734, degrees of freedom = 6, p = <0.05).

With respect to all parameters of size (Table 6), hornfels cores are largest at UPK9-10J2, and decline with distance from the river, albeit that the decline is quite small over the first 2 km to PL8. Silcrete follows the same trend, though the drop-off from UPK9-10J2 to PL8 is far more pronounced. Quartz blade cores follow no clear trend, though like those of hornfels and silcrete they are largest at UPK9-10J2.

Core reduction intensity can be examined through cortex retention and the number of flake scars observed. Cortex retention rates among hornfels blade cores generally decrease as distance to the river increases, though the difference between UPK9-10J2 and PL8 is not substantial (Fig. 8). The pattern for silcrete is somewhat more complicated, though as expected given its proximity to source, cortical silcrete blade cores are far more common at UPK9-10J2 than elsewhere in the catchment. Quartz generally reverses these trends, with the UPK9-10J2 blade cores, though the largest on average, typically having less cortex than those from the other sites.

With respect to flake scar counts, silcrete blade cores are more heavily reduced than those of other materials in all assemblages, with more than 75% of cores at most sites containing seven or more removals (Fig. 9). UPK9-10J2 is the exception, with half of all cores containing six or fewer removals. Other than this example, spatial trends in reduction intensity as measured by scar counts are either weak or non-existent for all raw materials examined.

Discussion

Previous research conducted in the Doring River catchment identified landscape-scale patterns in artifact manufacture and transport, allowing us to generate predictions regarding the expected character of Robberg assemblages on the Doring River itself (Low et al. 2017; Low & Mackay 2018). Specifically, they argued that the Doring River had been used as a staging point for the manufacture of large

TABLE 6 Metric comparisons for blade cores from UPK9-10J2, PL8, KFR, and MRS by raw material

Raw material	Site	N	Dist. to source (km)	Mass (g)			Length (mm)			Width (mm)			Thickness (mm)		
				Mean	SD	Median	Mean	SD	Median	Mean	SD	Median	Mean	SD	Median
Hornfels	UPK9	5†	0.2	28.2	27.4	20.4	44.9	11.5	44.4	31.3	13.4	29.6	14.8	5.9	18.9
	PL8	6	2	25.1	20.5	20.2	39.6	8.6	40.8	28.9	9.5	29.4	17.1	7.4	13.6
	KFR	5	13	5.5	6	2.7	26.1	7.9	23.7	16.1	6.9	12.8	8.9	2.9	9
	MRS	1	19	2.6	N/A	2.6	21.4	N/A	21.4	15.4	N/A	15.4	9.1	N/A	9.1
Quartz	UPK9	5	–‡	6.1	6.4	2	24.5	10.0	19.3	14.0	7.7	12.2	10.1	5.9	6.6
	PL8	24	0	1.1	1.7	0.7	15.2	4.7	13.9	8.9	4.4	7.4	5.5	2.9	4.9
	KFR	24	0	2	2.5	0.9	16.1	4.4	16	10.8	5.2	9.2	8.1	3.8	6.7
	MRS	46	0	2.1	2.5	1.3	16.8	5.2	17	11.5	4.4	10.9	8.1	4.1	7.3
Silcrete	UPK9	31	4.5	11.6	5.4	10.9	30.2	6.5	29.4	23.1	4.5	22.5	15.9	3.8	14.8
	PL8	17	31	6.2	3.1	5.4	25.9	5	26.3	19.8	4.6	19.4	12.4	2.9	13.4
	KFR	17	32	5.1	2.9	5.3	22.9	4.4	23.3	16.8	4.6	17.1	13.3	4.7	12.6
	MRS	26	26.5	4.7	3.4	4.1	22.6	5.4	22.4	16	4.4	15.9	11.5	4	11.4

† We exclude one core from calculation of mean and standard deviation in the hornfels group, due its outlying value (17 times higher than the next highest value).

‡ Location of quartz source is unknown.
All rock shelter sites are situated in locations where conglomerate beds crop out. There are no conglomerate beds at UPK9. Quartz is extremely rare in the proximate bedload of the river and the distance to its nearest source is unknown.

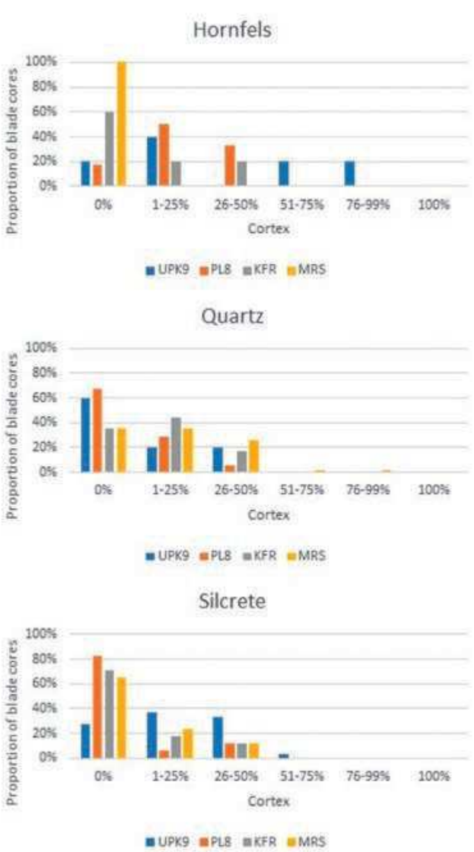

FIGURE 8 Cortex retention by raw material in complete blade cores at UPK9-10J2, PL8, KFR, and MRS

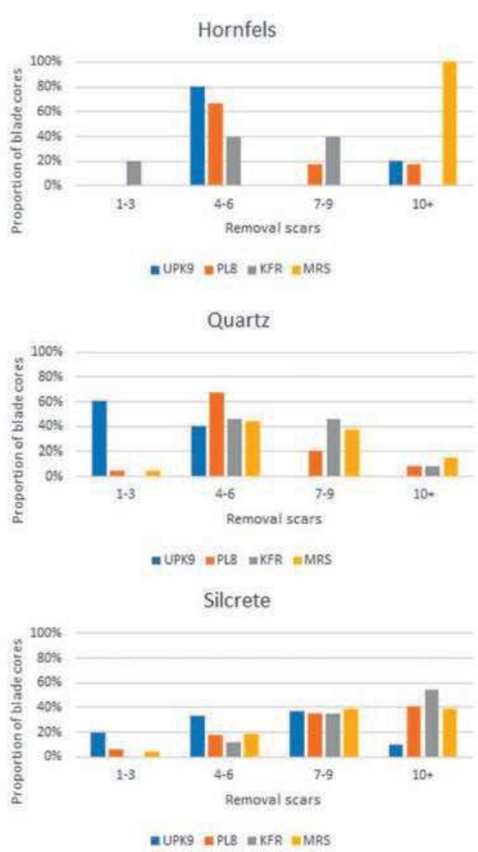

FIGURE 9 Number of removals on complete blade cores by raw material at UPK9-10J2, PL8, KFR, and MRS

numbers of silcrete and hornfels blades, and the preparation of silcrete cores for transportation into the wider catchment. They also implied that quartz would play a minor role in the Doring River assemblages relative to its abundance away from the river. The results from cluster UPK9-10J2 fit most of these expectations, with informative points of divergence.

The characteristics of the silcrete artifacts we examined were generally consistent with our hypothetical system of technological organization. Silcrete was a co-equal major contributor to the core assemblage at UPK9-10J2 and nearly all silcrete cores were used to manufacture blades. Three quarters of blade cores in the assemblage recorded are made from silcrete. Flakes and blades with primary and near-primary cortex, along with an abundance of overshot flakes, suggest some initial reduction of silcrete nodules occurred on site, with most of these nodules likely having been procured from the primary source at Swartvlei 4.5 km away. The silcrete cores in the UPK9-10J2 assemblage were also considerably larger than silcrete cores recorded elsewhere in the catchment, they retained more cortex, and they exhibited fewer removals, augmenting the previously observed decay pattern with distance from the Doring River. These indicators are consistent with the UPK9-10J2 assemblage representing an earlier stage in the silcrete reduction process than assemblages further from the river.

With some interesting exceptions, the character of quartz in the assemblage also broadly conforms to expectations. The paucity of quartz in the sample matches both the local absence of that lithology (the Doring River only cuts through quartz conglomerate beds of the Nardouw Formation downstream of PL8) and the trend of increasing proportional quartz abundance with distance from the river. Surprisingly, though, the quartz blade cores at UPK9-10J2 were anomalously large compared with those from our previously analyzed sites, which is not consistent with their introduction as heavily reduced pieces. It is possible these quartz pebbles and crystals were obtained opportunistically from isolated occurrences nearer to the site, but we have no evidence to support this. This aside, the low proportion of quartz in the assemblage is associated with an overall low prevalence of bipolar reduction, suggesting, in line with previous explanations, that use of bipolar reduction can be a situational response rather than an inherent property of the Robberg system (Pargeter 2017; Low & Mackay 2018).

The hornfels component of the UPK9-10J2 assemblage presents an interesting and somewhat complex picture. Hornfels is the single most common raw material in the sample, providing the largest number of artifacts in all classes. The vast majority of this hornfels was sourced from the river. However, while hornfels blades were numerous – consistent with our model of technological organization at the catchment scale – there was limited evidence for the cores that produced them. Only five of the 35 complete and broken hornfels cores retained any blade scars, and these were generally only a secondary product of the core. It is possible that these cores had been transformed into predominantly flake cores after initial production of blades, and that would be consistent with the large size of the hornfels blades in the assemblage and their elevated levels of cortex retention. However, the hornfels cores that produced blades at UPK9-10J2 were generally much smaller than those preserving only flake removals (Table 6), and thus cannot represent a more heavily reduced subset of that population. It is also possible that hornfels blade cores were removed from the assemblage for transport, yet at none of the other sites we have analyzed were hornfels blade cores common. This prompts the question of where, if the blade cores were transported away, were they ultimately discarded?

The similarities between hornfels blade cores at UPK9-10J2 and PL8, coupled with the differences between silcrete blade cores in those two samples, present a potential explanation for the observed pattern. PL8 is situated within 2 km of the Doring River, near the extensive cobble beds at the Doring/Putslaagte confluence. In respect of their abundance, average size, and cortical coverage the hornfels blade cores at UPK9-10J2 were nearly identical to those from PL8. Both the attribute data and reconstructed reduction systems from UPK9-10J2 suggests that blades were produced opportunistically from hornfels cores, rather than systematically. Because hornfels cobbles are abundant along the Doring River, such opportunistic production could be staged at any point along river, providing a regular supply of blades and flakes for transport into the wider catchment. The hornfels component of such a system could be quite difficult to identify in isolation on the river but would produce assemblages consistent with the identified signal of limited core transport, frequent flake and blade transport, and the rapid attenuation of hornfels abundance with distance from the Doring River.

The resource distribution, and thus organization, of silcrete procurement is different. While it can be found in cobble beds along the Doring River, secondary silcrete sources appear to have been exploited rarely during the Robberg. Opportunities for silcrete acquisition from primary sources are quite limited, with Swartvlei and Agtersfontein as the only two sources of which we presently know in the catchment. If primary reduction of material obtained from those sources took place in a few source-proximate locations on the Doring River, then we would expect a detectable increase in reduction with distance along the river as well as away from the river. This appears to be what we see at PL8 where, in contrast to hornfels blade cores, silcrete blade cores are already substantially reduced by the time they reach the site. Indeed, while there is a weak but clear signal of mass loss from PL8 to KFR to MRS, the total reduction in mean (1.5 g, or 14.2%) across those 17 km is swamped by the reduction from UPK9 to PL8 (5.4 g, or 46.6%). Consistent with the variable distribution of their sources, the hornfels and silcrete components of the Robberg system thus appear to have been organized quite differently.

This prospective difference in organization leads us to wonder whether hornfels and silcrete artifact manufacture were operationalized together or separately during the Robberg. During the ELSA at PL8, for example, we find evidence for blade manufacture on hornfels and bipolar reduction of very small quartz cores. Yet the open site evidence from UPK7 suggests that these two elements were enacted discretely; a ~30 ka sediment unit has produced substantial but wholly discrete assemblages of ELSA hornfels blade production (Low et al. 2017) and bipolar quartz flaking (Shaw et al. 2019).

Our sample is not without limitations. There are challenges inherent in working with small samples like the assemblage from UPK9-10J2; they may not represent the full range of technological variation and assemblage diversity is thus likely to be underestimated (Rhode 1988; Meltzer et al. 1992; Cochrane 2003). Acknowledging this, we chose to focus our analysis on the most common raw materials and lithic artifacts, and those least affected by our imposition of an arbitrary 20 mm size cut-off. An important counter-point here is that the archaeological record of southern Africa is dominated by surface assemblages generated at a range of scales, from those representing brief visits by one or a few individuals, to those representing either large group aggregations or repeated visitations (Shaw et al. 2019). If we constrain our work only to the largest aggregates, then we will necessarily produce an incomplete picture of past land use.

One final point we need to address concerns the likelihood and scale of mixing at UPK9-10J2. As noted at the outset, we selected that cluster for analysis due to limited evidence for older or younger material. While assemblages assigned to the subsequent Oakhurst and Wilton industries are common elsewhere at UPK9 (Shaw et al. 2019), they are not in evidence at UPK9-10J2. The results of our OSL analysis of the underlying sedimentary unit essentially precludes any contribution from older technocomplexes, and indeed that age at around the start of MIS 2 is what we would have expected for a sediment unit underlying a Robberg assemblage. Yet mixing is still a pertinent concern. First, there are numerous technological aspects of the last 27 ka in southern Africa that we do not understand and cannot characterize. Some of those could be over-printed on the Robberg at UPK9-10J2 and we would not know. It is possible that such overprint explains, for example, the hornfels component of the assemblage, though the very strong similarities with the dated assemblage from PL8 suggest that this is unlikely. Second, and more substantive, is the problem of mixing *within* the Robberg. As we have noted elsewhere, the technological character of the Robberg in the Doring River catchment changes through time, moving from silcrete-rich in the earlier phases to hornfels-rich in the later phases (Low 2019). Treating the Robberg as a singular entity thus necessitates conflating that variability, with the inevitability of signal-mixing. Thus, at UPK9-10J2, the hornfels, silcrete, and quartz components may have been formed at different times under different conditions. That is a possibility that we can neither ignore nor account for. We note though, that all assemblages are necessarily behavioral aggregates in which the actions undertaken across some unit of time are averaged (Bailey 2007), and that such averaging is sometimes beneficial to the identification of larger behavioral systems (Barton & Riel-Salvatore 2014).

Conclusions

The Robberg is the earliest coherent technocomplex of the LSA and one of the most recognizable within the culture history of southern Africa (Mitchell 1988; Wadley 1993; Lombard et al. 2012). However, this appearance of relative similarity across geographic and temporal scales has led to a lack of engagement with local and regional variation. Robberg technology in the Doring River catchment has been demonstrated here and in detailed comparisons with rock shelter assemblages (Low & Mackay 2018) to be highly responsive to local variation in raw material availability. Rather than reflecting the enactment of unvarying mental templates, technological organization within the Robberg documents complex, raw material-specific systems of tool production and transport. Our results further suggest that aspects of technology that become aggregated in rock shelter assemblages, such as the use of bipolar technology with quartz nodules, may be separated when sites in different landscape contexts are considered. Engaging with technological systems at a landscape level is vital for understanding the range of behaviors encompassed within those systems and is essential for understanding the way technology and information move across the landscape.

Acknowledgements

The Doring River Archaeology Project has been supported by grants from the Australian Research Council (DE130100068 & FT160100139) to AM. SW is supported by a National Science Foundation Graduate Research Fellowship (2017251536). Funding for sediment and OSL sampling and analysis was provided by a University of Wollongong PhD Scholarship to NP.

References

Aitken, M., 1985. Thermoluminescence dating. Academic Press Inc., London.

Ames, C., Chambers, S., Shaw, M., Phillips, N., Jones, B. G., Mackay, A., 2020a. Evaluating erosional impacts on open-air archaeological sites along the Doring River, South Africa: methods and implications for research prioritisation. Archaeological and Anthropological Sciences. 12(5).

Ames, C., Shaw, M., O'Driscoll, C., Mackay, A., 2020b. A Multi-User Mobile GIS Solution for Documenting Large Surface Scatters: An Example from the Doring River, South Africa. Journal of Field Archaeology. 45(6), 394-412.

Andrefsky, W., 1994. Raw-Material Availability and the Organization of Technology. American Antiquity. 59(1), 21-34.

Bader, G. D., Linstädter, J., Schoeman, M. H., 2020. Uncovering the Late Pleistocene LSA of Mpumalanga Province, South Africa: Early Results from Iron Pig Rock Shelter. Journal of African Archaeology. 18(1), 19-37.

Bailey, G., 2007. Time perspectives, palimpsests and the archaeology of time. Journal of Anthropological Archaeology. 26(2), 198-223.

Bamforth, D. B., 1991. Technological Organization and Hunter-Gatherer Land Use: A California Example. American Antiquity. 56(2), 216-234.

Barham, L. S., 1989. The Later Stone Age of Swaziland. University of Pennsylvania, Philadelphia.

Barton, C. M., Riel-Salvatore, J., 2014. The formation of lithic assemblages. Journal of Archaeological Science. 46, 334-352.

Boëda, E., Geneste, J.-M., Meignen, L., 1990. Identification de chaînes opératoires lithiques du Paléolithique ancien et moyen. Paléo, Revue d'Archéologie Préhistorique. 2, 43-80.

Bousman, C. B., Brink, J. S., 2018. The emergence, spread, and termination of the Early Later Stone Age event in South Africa and southern Namibia. Quaternary International, In Honour of James Brink. 495, 116-135.

Brennan, B. J., 2003. Beta doses to spherical grains. Radiation Measurements, Proceedings of the 10th international Conference on Luminescence and Electron-Spin Resonance Dating (LED 2002). 37, 299-303.

Chase, B. M., Faith, J. T., Mackay, A., Chevalier, M., Carr, A. S., Boom, A., Lim, S., Reimer, P. J., 2018. Climatic controls on Later Stone Age human adaptation in Africa's southern Cape. Journal of Human Evolution. 114, 35-44.

Cochrane, G. W. G., 2003. Artefact attribute richness and sample size adequacy. Journal of Archaeological Science. 30(7), 837-848.

Deacon, J., 1978. Changing patterns in the late Pleistocene/early Holocene prehistory of Southern Africa as seen from the Nelson Bay Cave Stone artifact sequence. Quaternary Research. 10(1), 84-111.

Deacon, J., 1982. The Later Stone Age in the southern Cape, South Africa (PhD thesis). University of Stellenbosch.

Deacon, J., 1984. The later stone age of southernmost Africa. BAR.

Galbraith, R. F., Roberts, R. G., Laslett, G. M., Yoshida, H., Olley, J. M., 1999. Optical Dating of Single and Multiple Grains of Quartz from Jinmium Rock Shelter, Northern Australia: Part I, Experimental Design and Statistical Models. Archaeometry. 41(2), 339-364.

Jacobs, Z., Roberts, R. G., 2017. Single-grain OSL chronologies for the Still Bay and Howieson's Poort industries and the transition between them: Further analyses and statistical modelling. Journal of Human Evolution. 107, 1-13.

Kuhn, S. L., 1992. On Planning and Curated Technologies in the Middle Paleolithic. Journal of Anthropological Research. 48(3), 185-214.

Kuhn, S. L., 1995. Mousterian Lithic Technology: An Ecological Perspective. Princeton University Press.

Leroi-Gourhan, A., 1964. Le geste et la parole. I: Technique et language. Albin Michel.

Leroi-Gourhan, A., 1965. Le geste et la parole. II: La mémoire et les rythmes. Albin Michel.

Loftus, E., Sealy, J., Lee-Thorp, J., 2016. New Radiocarbon Dates and Bayesian Models for Nelson Bay Cave and Byneskranskop 1: Implications for the South African Later Stone Age Sequence. Radiocarbon. 58(2), 365-381.

Lombard, M., Wadley, L., Deacon, J., Wurz, S., Parsons, I., Mohapi, M., Swart, J., Mitchell, P., 2012. South African and Lesotho Stone Age sequence updated. The South African Archaeological Bulletin. 67(195), 123-144.

Low, M., 2019. Continuity, Variability and the Nature of Technological Change During the Late Pleistocene at

Klipfonteinrand Rockshelter in the Western Cape, South Africa. African Archaeological Review. 36, 67-88.

Low, M., Mackay, A., 2016. The late Pleistocene microlithic at Putslaagte 8 Rockshelter in the Western Cape, South Africa. South African Archaeological Bulletin. 71(204), 146.

Low, M., Mackay, A., 2018. The Organisation of Late Pleistocene Robberg Blade Technology in the Doring River Catchment, South Africa. Journal of African Archaeology. 16(2), 168-192.

Low, M., Mackay, A., Phillips, N., 2017. Understanding Early Later Stone Age technology at a landscape-scale: evidence from the open-air locality Uitspankraal 7 (UPK7) in the Western Cape, South Africa. Azania: Archaeological Research in Africa. 52(3), 1-34.

Mackay, A., Cartwright, C. R., Heinrich, S., Low, M. A., Stahlschmidt, M. C., Steele, T. E., 2020. Excavations at Klipfonteinrand reveal local and regional patterns of adaptation and interaction through MIS 2 in southern Africa. Journal of Paleolithic Archaeology. 3, 1-36.

Mejdahl, V., 1979. Thermoluminescence Dating: Beta-Dose Attenuation in Quartz Grains. Archaeometry. 21(1), 61-72.

Meltzer, D. J., Leonard, R. D., Stratton, S. K., 1992. The relationship between sample size and diversity in archaeological assemblages. Journal of Archaeological Science. 19(4), 375-387.

Mitchell, P., 1988. The late Pleistocene early microlithic assemblages of southern Africa. World Archaeology. 20(1), 27-39.

Mitchell, P. J., 1995. Revisiting the Robberg: New Results and a Revision of Old Ideas at Sehonghong Rock Shelter, Lesotho. The South African Archaeological Bulletin. 50(161), 28-38.

Mitchell, P. J., 1996. The late Quaternary of the Lesotho highlands, southern Africa: Preliminary results and future potential of ongoing research at Sehonghong shelter. Quaternary International. 33, 35-43.

Mitchell, P. J., 2000. The Organization of Later Stone Age Lithic Technology in the Caledon Valley, Southern Africa. African Archaeological Review. 17, 141-176.

Murray, A. S., Wintle, A. G., 2000. Luminescence dating of quartz using an improved single-aliquot regenerative-dose protocol. Radiation Measurements. 32(1), 57-73.

Nelson, M. C., 1991. The Study of Technological Organization. Archaeological Method and Theory. 3, 57-100.

Pargeter, J., 2016. Lithic miniaturization in Late Pleistocene southern Africa. Journal of Archaeological Science: Reports. 10, 221-236.

Pargeter, J., 2017. Lithic miniaturization in Late Pleistocene Southern Africa (Ph.D. thesis). Stony Brook University.

Pargeter, J., Loftus, E., Mackay, A., Mitchell, P., Stewart, B., 2018. New ages from Boomplaas Cave, South Africa, provide increased resolution on late/terminal Pleistocene human behavioural variability. Azania: Archaeological Research in Africa. 53(2), 156-184.

Pargeter, J., Loftus, E., Mitchell, P., 2017. New ages from Sehonghong rock shelter: Implications for the late Pleistocene occupation of highland Lesotho. Journal of Archaeological Science: Reports. 12, 307-315.

Pargeter, J., Redondo, M., 2016. Contextual approaches to studying unretouched bladelets: A late Pleistocene case study at Sehonghong Rockshelter, Lesotho. Quaternary International, The African Quaternary: environments, ecology and humans Inaugural AFQUA conference. 404, 30-43.

Phillips, N., Pargeter, J., Low, M., Mackay, A., 2019. Open-air preservation of miniaturised lithics: experimental research in the Cederberg Mountains, southern Africa. Archaeological and Anthropological Sciences. 11, 5851-5877.

Porraz, G., Igreja, M., Schmidt, P., Parkington, J. E., 2016. A shape to the microlithic Robberg from Elands Bay Cave (South Africa). Southern African Humanities. 29(1), 203-247.

Prescott, J. R., Hutton, J. T., 1994. Cosmic ray contributions to dose rates for luminescence and ESR dating: Large depths and long-term time variations. Radiation Measurements. 23(2-3), 497-500.

Rhode, D., 1988. Measurement of Archaeological Diversity and the Sample-Size Effect. American Antiquity. 53(4), 708-716.

Rousseeuw, P. J., Debruyne, M., Engelen, S., Hubert, M., 2006. Robustness and Outlier Detection in Chemometrics. Critical Reviews in Analytical Chemistry. 36(3-4), 221-242.

Shaw, M., Ames, C., Phillips, N., Chambers, S., Dosseto, A., Douglass, M., Goble, R., Jacobs, Z., Jones, B., Lin, S., Low, M., McNeil, J.-L., Nasoordeen, S., O'Driscoll, C., Saktura, R., Sumner, A., Watson, S., Will, M., Mackay, A., 2019. The Doring River Archaeology Project: Approaching the evolution of human land use patterns in the Western Cape, South Africa. PalaeoAnthropology. 400, 422.

Tixier, J., 1980. Préhistoire et technologie lithique, 1.

Villa, P., Soriano, S., Tsanova, T., Degano, I., Higham, T. F. G., d'Errico, F., Backwell, L., Lucejko, J. J., Colombini, M. P., Beaumont, P. B., 2012. Border Cave and the beginning of the Later Stone Age in South Africa. Proceedings of the National Academy of Sciences. 109(33), 13208-13213.

Vogel, J. C., Fuls, A., Visser, E., 1986. Pretoria Radiocarbon Dates III. Radiocarbon. 28, 1133-1172.

Wadley, L., 1993. The Pleistocene Later Stone Age south of the Limpopo River. Journal of World Prehistory. 7, 243-296.

Wilkins, J., Brown, K. S., Oestmo, S., Pereira, T., Ranhorn, K. L., Schoville, B. J., Marean, C. W., 2017. Lithic technological responses to Late Pleistocene glacial cycling at Pinnacle Point Site 5-6, South Africa. PLOS ONE. 12(3), e0174051.

Will, M., Mackay, A., Phillips, N., 2015. Implications of Nubian-Like Core Reduction Systems in Southern Africa for the

Identification of Early Modern Human Dispersals. PLOS ONE. 10(6), e0131824.
Wintle, A. G., 1997. Luminescence dating: laboratory procedures and protocols. Radiation Measurements. 27(5-6), 769-817.
Wood, R., Jacobs, Z., Vannieuwenhuyse, D., Balme, J., O'Connor, S., Whitau, R., 2016. Towards an Accurate and Precise Chronology for the Colonization of Australia: The Example of Riwi, Kimberley, Western Australia. PLOS ONE. 11(19), e0160123.